Vulcanization: New Focus on a Traditional Technology by Small-Angle Neutron Scattering

Yuko Ikeda,* Norihito Higashitani, Kensuke Hijikata, Yota Kokubo, and Yuichi Morita

Graduate School of Science and Technology, Kyoto Institute of Technology, Matsugasaki, Sakyo, Kyoto 606-8585, Japan

Mitsuhiro Shibayama, Noboru Osaka, Takuya Suzuki, and Hitoshi Endo

Institute for Solid State Physics, The University of Tokyo, Kashiwa, Chiba 277-8581, Japan

Shinzo Kohjiya

Department of Chemistry, Faculty of Science (SC4-303), Mahidol University, Salaya Campus Phuthamonthon, Nakorn Pathom 73170, Thailand

Received December 6, 2008; Revised Manuscript Received February 6, 2009

ABSTRACT: Vulcanization is the most important and conventional process in preparing rubber products. Network structure in the vulcanizates has been assumed to dominantly determine their physical properties together with network-chain density. Therefore, control of network structure in the vulcanizates is of at most importance for a fundamental design of rubber products. However, inhomogeneity of the network structure has not been much elucidated in spite of the long history of vulcanization since 1839, due to the complicated reactions among rubber and cross-linking reagents. Here, we look more closely at vulcanization and show its new role to control the network inhomogeneity on the basis of small-angle neutron scattering analysis of vulcanized rubbers. Combination and composition of the cross-linking reagents, especially those of zinc oxide with the other reagents, were found to be crucial for the control. A characteristic feature of strain-induced crystallization of the vulcanizates is also accounted for by the notion of network inhomogeneity. These results will be useful for further enhancing the technological potential of the traditional yet indispensable vulcanization.

Introduction

Vulcanization is one of the most traditional chemical processes in polymer industries.[1−3] Almost all rubber products, such as pneumatic tires of automobiles and airplanes, are manufactured using vulcanization (cross-linking reactions by sulfur). Since the discovery of using sulfur by Goodyear in 1839, sulfur cross-linking reactions have been advanced by ceaseless innovation of accelerators, activators, retarders, and so on, in order to improve processability and mechanical properties.[1−5] However, the mechanism of vulcanization has not been conclusively clarified yet, due to complicated chemical reactions between rubber, elemental sulfur, and other cross-linking reagents at each processing step. Up to now, most vulcanization systems have been developed by skillful and elaborate techniques based on the trial-and-error method.

In the community of rubber technologists, complexity of the vulcanization has intuitively been accepted to give a heterogeneous network structure, and the inhomogeneity in cross-linked rubbers has been a difficult yet challenging problem in polymer science.[2,6,7] Homogeneous or heterogeneous: which kind of processing is better for desired properties? How does one control the heterogeneity of rubber mix during processing? Ultimately, what kind of network structure is the best for producing high-performance rubber materials? In order to answer these questions, identification of the inhomogeneity in the cross-linked rubbers is a very important subject not only from the strong demand for a rational product design but also from the academic interests.

Small-angle neutron scattering (SANS) has been one of the powerful tools since its first application to a structural study in polymer science.[8] Both hydrogen/deuterium labeling and hydrogen/deuterium contrast-matching techniques allow us to determine the size, orientation, and conformation of target polymer chains,[7,9] and the elucidation of polymer network homogeneity has become an important issue for SANS more recently.[7] However, we can hardly find a systematic study on network inhomogeneity in sulfur cross-linked rubbers.

In this study, isoprene rubber (IR), a synthetic analog of natural rubber (NR), was sulfur cross-linked, and the swollen IRs in deuterated toluene (*d*-toluene) were used for SANS measurements to elucidate the network inhomogeneity and local network structure. The reason of using not NR but IR as rubber is based on the fact that the nonrubber components in NR such as proteins and lipids[10,11] gave an additional scattering in the SANS profile,[12] which made the analysis difficult by overlapping with the scattering ascribable to inhomogeneity.[6,7,13,14] Invisible inhomogeneity in cross-linked rubbers can be visualized by swelling similarly as is the case in polymer gels.[7,15] In fact, various homogeneous and heterogeneous networks were studied by SANS using deuterated solvents.[16−19] A new role of vulcanization that controls the network inhomogeneity is shown here. Additionally, effects of the network inhomogeneity are studied on strain-induced crystallization (SIC) behaviors of the cross-linked IR as revealed by simultaneous time-resolved wide-angle X-ray diffraction (WAXD) and tensile measurements using a synchrotron radiation system at SPring-8.[20−24]

Experimental Section

Materials. Isoprene rubber (IR 2200) was supplied from JSR Co. Elemental sulfur (powder, 150 mesh), stearic acid (LUNAC S-25), zinc oxide (average diameter: 0.29 μm[25]), and *N*-cyclohexyl-2-benzothiazole sulfenamide (CBS, Sanceler CM-G) were commercial grades for rubber processing and used as received. They

* Corresponding author. Telephone: +81 75 724 7558. Fax: +81 75 724 7558. E-mail: yuko@kit.ac.jp.

10.1021/ma802730z CCC: $40.75
Published on Web 03/16/2009

Table 1. Recipes for Preparation and Properties of IR Vulcanizates

	IR[a]	stearic acid (phr[b])	ZnO[c] (phr)	CBS[d] (phr)	sulfur (phr)	g[e]	Q[f]	$\nu' \times 10^4$ (mol cm^{-3})[g]	$\nu \times 10^4$ (mol cm^{-3})[h]	$\xi^{i,j}$ (nm)	$\Xi^{k,j}$ (nm)	$\xi^{i,l}$ (nm)	$\Xi^{k,l}$ (nm)[l]
						Series 1							
IR-1-Z1-S1	100	2.0	1.0	0.67	1.0	0.97	6.7	0.784	0.814	3.12	19.0	3.60	19.8
IR-1-Z1-S1.5	100	2.0	1.0	1.0	1.5	0.97	6.0	0.992	1.05	3.19	30.9	3.58	30.9
IR-1-Z1-S3	100	2.0	1.0	2.0	3.0	0.96	5.6	1.16	1.24	3.25	59.8	3.55	59.9
IR-1-Z1-S4.5	100	2.0	1.0	3.0	4.5	0.94	5.5	1.26	1.33	3.22	91.5	3.60	91.6
						Series 2							
IR-2-Z0-St2	100	2.0	0.0	1.0	1.5	0.90	18	0.117	0.143	4.14	42.5	4.87	42.0
IR-2-Z0.5-St2	100	2.0	0.5	1.0	1.5	0.95	7.9	0.556	0.594	3.67	54.2	4.02	54.4
IR-2-Z1-St2	100	2.0	1.0	1.0	1.5	0.97	6.0	0.992	1.05	3.19	30.9	3.58	30.9
IR-2-Z2-St2	100	2.0	2.0	1.0	1.5	0.97	5.6	1.14	1.49	2.28	18.8	2.66	19.0
IR-2-Z4-St2	100	2.0	4.0	1.0	1.5	0.97	6.1	0.966	1.35	2.26	18.1	2.69	18.3
						Series 3							
IR-3-Z1-St0	100	0.0	1.0	1.0	1.5	0.98	5.9	1.01	1.14	3.46	52.2	4.00	53.0
IR-3-Z2-St0	100	0.0	2.0	1.0	1.5	0.98	5.9	1.03	1.11	3.46	53.8	4.06	57.2
IR-3-Z4-St0	100	0.0	4.0	1.0	1.5	0.98	5.9	1.04	1.17	3.39	62.0	4.02	67.5

[a] Isoprene rubber (IR 2200). [b] Parts per one hundred rubber by weight. [c] Zinc oxide. [d] Accelerator: *N*-cyclohexyl-2-benzothiazole sulfenamide (CBS). [e] Gel fraction. [f] Degree of equilibrium swelling by volume in toluene at 25 °C. [g] Network-chain density determined by swelling experiment. [h] Network-chain density determined by tensile experiment. [i] Mesh size. [j] The incoherent subtraction was conducted by curve fitting. [k] Size of network domain. [l] The incoherent subtraction was conducted by a method using a transmission of neutron beam from a sample in a quartz cell.,[29]

were supplied from Hosoi Chemical Industry Co. Ltd., Kao Co., Sakai Chemical Industry Co. Ltd., and Sanshin Chemical Industry Co. Ltd., respectively. According to the recipes shown in Table 1, IR compounds were prepared by a conventional mixing on a two-roll mill, and were subject to cross-linking by compression molding at 140 °C for 30 min to obtain IR vulcanizates of 1 mm thickness. Note as shown in Table 1 that in series 1 the concentarations of sulfur and accelerator were changed with keeping the ratio of them constant in the presence of stearic acid and ZnO. (Both are called "activator" or "auxiliary accelerator" in the rubber industry.) In series 2 the concentarations of ZnO were changed in the presence of stearic acid, and in series 3 in the absence of stearic acid. (Traditional rubber technologists have never thought of vulcanization without stearic acid. However, it was recently reported that it was fully possible.[26] Under the absence of both stearic acid and ZnO, the vulcanization was agonizingly slow.) The figures in the table are in phr, which stands for "parts per one hundred rubber by weight".

Swelling Measurement. The sample specimens, whose sizes are ca. 5 mm × ca. 7 mm × ca. 1 mm, were swollen in large amount of toluene at 25 °C for over 3 h to their equilibrium swelling, and their volume change was measured using CCD camera (VC1000 Digital Fine Scope, OMRON Co.). The degree of equilibrium swelling by volume, Q, of the vulcanizates was calculated using the equation ($Q = (V_s/V_0)$), where V_0 and V_s are the volumes before and after swelling, respectively.

Small-Angle Neutron Scattering (SANS) Meaurement. SANS measurements were carried out at two-dimensional SANS instrument, SANS-U, Institute for Solid State Physics, The University of Tokyo, located at JRR-3 Research Rector, Japan Atomic Energy, Tokai, Ibaraki, Japan. A monochromated cold neutron beam with the average neutron wavelength of 0.70 nm and 10% wavelength distribution was irradiated to the samples. The scattered neutrons were counted with a two-dimensional position detector (Ordela 2660N, Ork Ridge, USA.) The sample-to-detector distances were chosen to be 2.00 and 8.00 m. After necessary corrections for open beam scattering, transmission and detector inhomogeneities, the corrected scattering intensity functions were normalized to the absolute intensity scale with a polyethylene secondary standard. The details of the instrument and data reduction are given elsewhere.[27,28] Incoherent subtraction was conducted both by curve fitting and a method to use the transmission proposed by Shibayama et al.[29] The incoherent scattering intensity was estimated by the neutron transmission (hereafter we call the transmission method) via $I_{inc} \approx \mu(e^{\mu t} - 1)/(4\pi\mu t)$, where μ [cm^{-1}] is the linear absorbance defined by $\mu = -e^T/t$. Here, T is the transmission of neutron beam and t [cm] is the sample thickness. Deuterated toluene was used for swelling the sample to be subjected to SANS measurement at the equilibrium of swelling.

Simultaneous Wide-Angle X-ray Diffraction (WAXD) and Tensile Measurement. Synchrotron WAXD measurements were carried out at BL-40XU beam line of SPring-8 in Harima, Japan.[20] A custom-made tensile tester was situated on the beam line and WAXD patterns were recorded during tensile measurement at room temperature (ca. 25 °C). The wavelength of the X-ray was 0.08322 nm and the camera length was 0.197 m, which was determined by using lead stearate as a standard sample. The two-dimensional WAXD patterns were recorded using a CCD camera (HAMAMATSU C4880−50). Intensity of the incident X-ray was attenuated using a rotating slit equipped on the beam line and the incident beam was exposed on the sample for 50 ms every 6 s in order to avoid radiation damage of the specimens and to minimize the relaxation effect for SIC measurement. The absorption correction for thinning of the samples was carried out using calculated correction coefficient, which was obtained by using absorption coefficients per density[30] and weight fractions for each element in the samples, assuming the affine deformation of the rubber samples. Here, the Poisson ratio of 0.50 was used since the measured ones for all samples were 0.492−0.499. The custom-made tensile tester (ISUT-2201, Aiesu Giken, Co., Kyoto) could stretch the specimen symmetrically to examine the same position of the specimen by X-ray diffraction/scattering during the deformation. Ring-shaped samples were subjected to the tensile measurement in order to correctly measure the stretching ratio (α) of deformed samples. The inner and outer diameters of ring-shaped specimen were 11.7 and 13.7 mm, respectively. Here, α is defined as $\alpha = l/l_0$, in which l_0 is the initial length and l is the length after deformation. The stretching speed was 100 mm min^{-1}, i.e., strain speed was ca. 4.98 min^{-1}. The obtained WAXD images were processed using "POLAR" (Stonybrook Technology & Applied Research, Inc.).[31−33] The WAXD patterns of stretched samples were decomposed into three components, i.e., isotropic, oriented amorphous and crystalline components. Three components were azimuthally integrated within the range of ±75° from the equator: The details of this analytical method were described in our previous paper.[33] The "crystallinity index (CI)" was determined by eq 1.

$$\mathrm{CI} = \frac{\sum_{\text{crystal}} 2\pi \int \sin\phi \, \mathrm{d}\phi \int I(s)s^2 \, \mathrm{d}s}{\sum_{\text{total}} 2\pi \int \sin\phi \, \mathrm{d}\phi \int I(s)s^2 \, \mathrm{d}s} \quad (1)$$

In eq 1, $I(s)$ represents the intensity distribution of each peak that is read out from the WAXD pattern, s is the radial coordinate

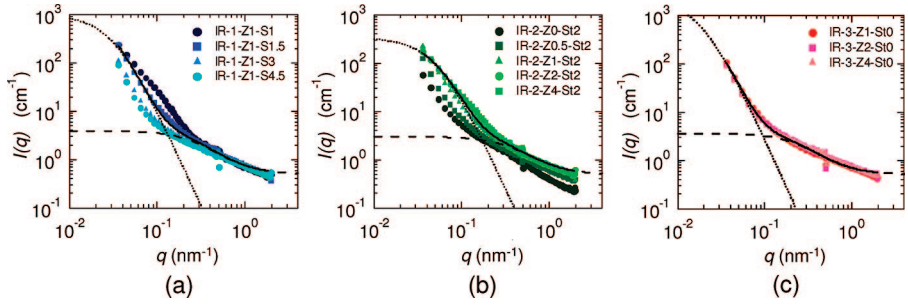

Figure 1. SANS intensity functions of IR vulcanizates: (a) series 1; (b) series 2; (c) series 3. For the sample codes, refer to Table 1. The dotted and dashed lines are the fit with eq 4 for IR-1-Z1-S1, IR-2-Z2-St2, and IR-3-Z2-St0, respectively.

in reciprocal space in nm^{-1} unit ($s = 2(\sin\theta/\lambda)$, where λ is the wavelength and 2θ is the scattering angle), and ϕ is the angle between the scattering vector of the peak and the fiber direction.

Measurement of Network-Chain Density. Using Q values measured by swelling, network-chain density (ν') of swollen vulcanizates was determined by the modified Flory−Rehner equation[34]

$$\nu' = -\frac{1}{V}\left[\frac{\ln(1 - V_R) + V_R + \chi V_R^2}{g^{2/3}V_R^{1/3} - V_R/2}\right] \quad (2)$$

where V_R is the volume fraction of the vulcanizate in the swollen sample, V is the molar volume of the solvent, and χ is the Flory−Huggins interaction parameter. The χ used in the calculations was 0.39.[35,36] Since the vulcanizates were prepared by a conventional processing in rubber science and technology, a gel fraction (g) in a network was taken into account for the measurement. The gel fraction (insoluble part) in the vulcanizate was determined by "$g = W_1/W_0$", where W_0 and W_1 are the weights before swelling and after drying the swollen sample, respectively. Gel fractions of all the samples were larger than 0.94 except the vulcanizate without mixing ZnO (0.90) as shown in Table 1, implying that the network formation in the most samples were approximately complete under the preparation conditions.

The network-chain density (ν) of the dry samples was also estimated from the tensile properties measured by a simultaneous WAXD and tensile measurement using the equation of the classical theory of rubber elasticity[37]

$$\sigma = \nu kT(\alpha - /1\alpha^2) \quad (3)$$

where σ is the stress, k is the Boltzmann constant, and T is absolute temperature. α is the stretching ratio. Their network-chain densities estimated by two different calculations have a good correlation.

Results and Discussion

SANS Profiles and a Two-Phase Model. Figure 1 shows double logarithmic plots of SANS intensities as a function of the magnitude of the scattering wave vector, $q \equiv |\mathbf{q}|$, in d-toluene at 25 °C for the three series of cross-linked IR having various network-chain densities. All SANS profiles clearly show an upturn scattering in the smaller-angle regions ($q \leq 0.2$ nm), suggesting the presence of inhomogeneity in the network structure.[6,7,12−14] In the larger-angle regions ($q > 0.2$ nm^{-1}), it is observed that the SANS profiles in series 1 were almost equal regardless of their different network-chain densities, whereas those in series 2 are dependent on the amount of ZnO. The SANS profiles in both regions of series 3, however, were very similar regardless of the variation of ZnO.

These SANS results suggest the presence of heterogeneous structures in all the samples, but the details in their inhomogeneity may be different depending on the recipes for the vulcanization (Table 1). In order to analyze these SANS profiles quantitatively, a series of curve fitting were conducted with a scattering function for swollen gels: Normally, an observed scattering intensity $I(q)$ of inhomogeneous swollen gels can be described by a sum of the scattered intensity from the corresponding polymer solution $I_{soln}(q)$ and those of the excess scattering $I_{ex}(q)$ and incoherent scattering I_{inc} over a wide range of q given by

$$I(q) = I_{soln}(q) + I_{ex}(q) + I_{inc} \quad (4)$$

For the swollen gels, the scattered intensity from a corresponding polymer solution $I_{soln}(q)$ is given by a Lorentz (L) function[38] in the long wavelength limit,

$$I_{soln}(q) = I_{soln}(0)/(1 + \xi^2 q^2) \quad (5)$$

where ξ is the correlation length, i.e., blob size (mesh size of network).[39−44]

On the other hand, a squared-Lorentz function (SL-function) was employed for $I_{ex}(q)$ in this study in order to describe solid-like inhomogeneity in the gel,[45,46] as the most suitable scattering function for swollen gels.[12]

$$I_{ex}(q) = I_{ex}(0)/(1 + \Xi^2 q^2)^2 \quad (6)$$

Here, Ξ is a characteristic length scale (chord length) of solid-like inhomogeneity. The SL-function is the so-called Debye−Bueche function.[47] which is often used to represent cross-link (or structure) inhomogeneity in polymer gels.[7,9,12,15]

In this study, the inhomogeneous network structure of swollen IR is speculated as schematically shown in Figure 2a. This is a two-phase model network, where domains of high network-chain density (B phase, dispersed) are embedded in rubbery network matrix (A phase, continuous). Recently, this two-phase structure was proposed for cross-linked NR to explain its SIC behavior.[24] A similar model was reported by Fujimoto[48] as early as in 1960s. Curve fittings of all observed SANS profiles by a combination of L-function and SL-function with the incoherent scattering intensity were quite successful: For examples, the fitted lines for IR-1-Z1-S1, IR-2-Z2-St2, and IR-3-Z2-St0 are displayed by dotted lines in Figure 1a,b,c, respectively. The fittings with eq 4 in all SANS profiles allowed us to obtain the structural parameters (ξ and Ξ) of swollen IR vulcanizates shown in Figure 2b. Note that the cartoons are drawn in order to emphasize the only difference in the degrees of cross-linking between rubber matrix and network domains. One example of realistically displayed two-phase network structures is also shown in Figure 2c, although the distance between the domains is not revealed.

All structural parameters are summarized in Table 1. The evaluated incoherent scattering intensity by curve fitting was around 0.4 cm^{-1} (for samples with $V_R \approx 0.15$) except for IR-2-Z0-St2 ($I_{inc} = 0.19$ cm^{-1}; a highly swollen sample, $V_R \approx 0.05$), which is reasonable for polymer-deuterated toluene solutions and showed a systematic variation as a function of polymer concentration. The incoherent scattering intensity estimated by

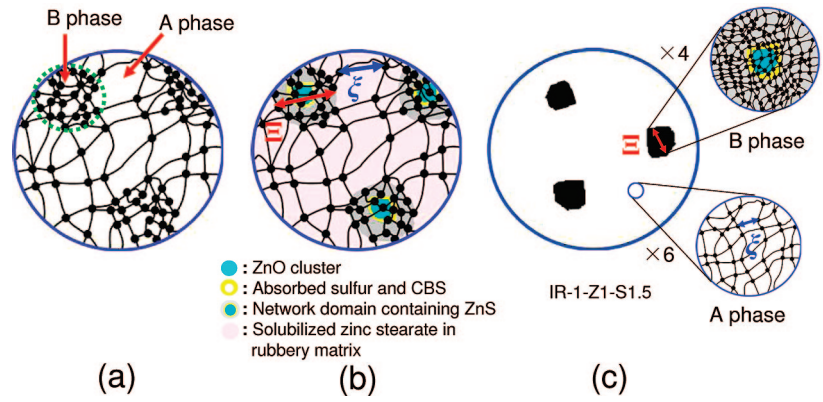

Figure 2. Proposed models to explain the inhomogeneity of network structure in IR vulcanizate. (a) Two-phase model of network structure: A phase, matrix with low network-chain density; B phase, network domain with high network-chain density. (b) Inhomogeneity around ZnO clusters in the matrix, where mesh size (ξ) and size of network domain (Ξ) are also displayed. ξ and Ξ should be referred to the measured ξ and Ξ shown in Table 1. (c) One example of two-phase network structure with a high reality, although the distance between the domains is not revealed yet.

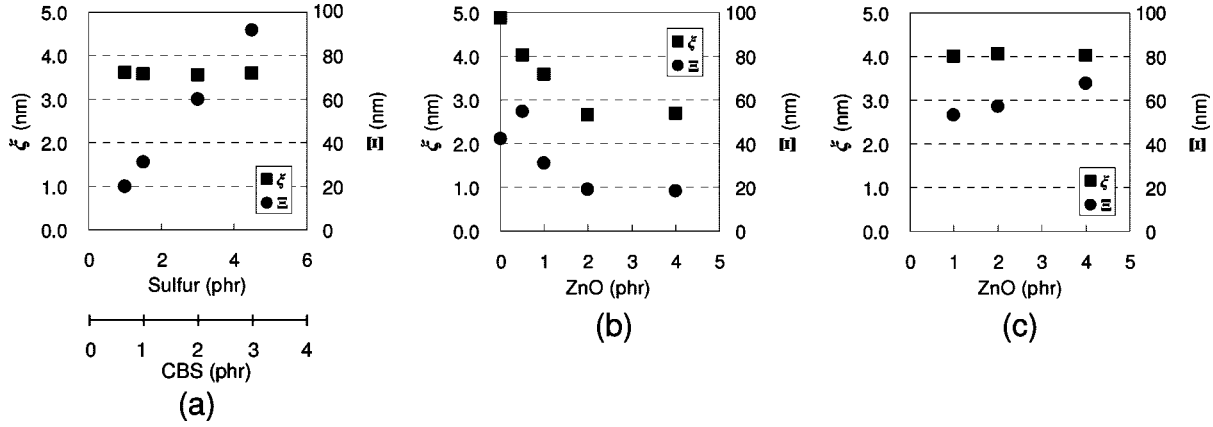

Figure 3. Effect of sulfur cross-linking reagents on mesh size (ξ) and size of network domain (Ξ). (a) Dependence of ξ and Ξ on sulfur and accelerator of series 1. (b) Dependence of ξ and Ξ on ZnO of series 2. (c) Dependence of ξ and Ξ on ZnO of series 3.

the transmission method was around 0.5 cm^{-1} except for IR-2-Z0-St2 (I_{inc} = 0.37 cm^{-1}). Since the incoherent subtraction by the latter is more reproducible and accurate,[29] the obtained structural parameters by this method are discussed in the following sections.

Effect of Sulfur. Figure 3a shows the plots of the mesh size (ξ) in the rubbery matrix and the size of network domain (Ξ) against the concentrations of sulfur and accelerator for series 1. It is surprising that mesh sizes of the cross-linked rubbers of series 1 is independent of sulfur and accelerator concentrations (the ratio of the two is constant), while the Ξ values are clearly dependent on them. Since the network-chain densities of these samples were varied by the concentrations of sulfur (together with the accelerator), this result means that the mesh sizes in the rubbery matrix were almost the same regardless of the network-chain density (which is an overall value) and did not depend on the concentrations of sulfur and accelerator when of the concentrations of stearic acid and ZnO were fixed. The invariance of the mesh size in series 1 is explained by a known phenomenon that stearic acid reacts with ZnO to form zinc stearate,[1,4,5] which is dissolved in the rubbery matrix[49] and this species is important for sulfur cross-linking reaction.[1−5,49,50] Namely, the generated amounts of zinc stearate in the rubbery matrix are expected to be almost equal among the samples of series 1, when the compounds are prepared according to the recipe shown in Table 1, followed by the compression molding at 140 °C for 30 min.

Different from the mesh size, the size of network domain (Ξ) of series 1 was found to linearly increase by increasing the concentration of sulfur and accelerator as shown in Figure 3a. In other words, the size of network domains was increased by increasing the network-chain density. This finding may be explained by the absorption of sulfur and accelerator onto ZnO particles or its clusters. For example, ZnO surface is reported to function as a reaction site of sulfur cross-linking reactions by bringing the reactants together.[51] Additionally, sulfur and sulfur donors including accelerators were reported to be strongly adsorbed on the surface of ZnO clusters, [52] which was suggested by computation on the basis of the density functional theory. On the surface, a presumably "chelate-type" complex of Zn was generated and was assumed to be responsible for activation of elemental sulfur during vulcanization.[4,50,52] In addition, the accelerated vulcanization with ZnO was also reported not to occur uniformly in the rubbery matrix but to occur around ZnO particles, which was estimated from the results of energy-filtering transmission electron microscopy.[53,54] Therefore, the amounts of adsorbed sulfur and CBS (the accelerator, see Table 1) on each ZnO cluster were estimated to be increased by increasing their mixed amounts in series 1, while the concentrations of stearic acid and ZnO were fixed. As a result, the degree of sulfur cross-linking reaction around the ZnO clusters must have been larger by increasing sulfur and CBS, which has brought about the increase of network domain size. These observations on ξ and Ξ have never been reported before, as far as we know.

Role of Zinc Oxide. ZnO has been recognized to be an important component for sulfur cross-linking reaction, but the exact role of ZnO on the network structure has not been well

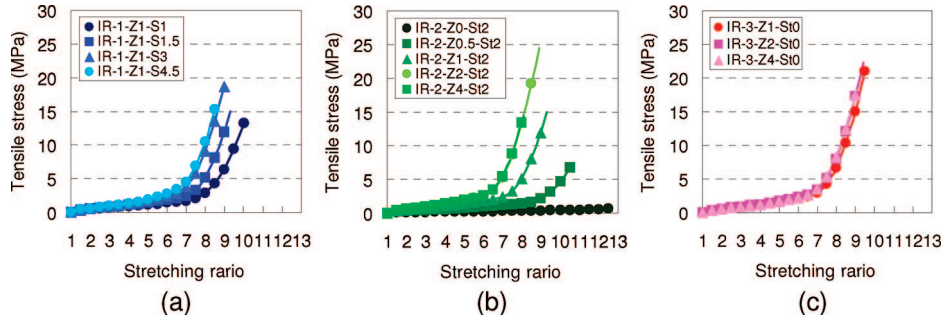

Figure 4. Tensile stress−strain curves of IR vulcanizates: (a) series 1, (b) series 2, and (c) series 3 samples.

understood. Figure 3b gives us an interesting finding on the effects of ZnO on the vulcanization. Variations of ξ and Ξ by the concentration of ZnO are shown in Figure 3b for series 2. It is worth noting that ξ and Ξ linearly decreased more or less by increasing the concentrations of ZnO in the region from 0.5 phr to 2.0 phr in the presence of 2.0 phr stearic acid. However, both ξ and Ξ values were similar between the samples mixed with ZnO of 2.0 phr and 4.0 phr, *i.e.*, use of an excess of ZnO (4.0 phr) did not much affect both ξ and Ξ. In addition to these observations, the variation of ξ and Ξ in series 3, where stearic acid was not present, was found to be small as shown in Figure 3c. These results clearly suggest that ZnO plays an important role in combination with stearic acid, in controlling not only the mesh size but also the size of network domain in the cross-linked rubber. In other words, vulcanization reactions were activated by ZnO (the naming "activator" is correct!) in the presence of stearic acid. As a role of stearic acid, it was also found to effectively disperse ZnO particles in rubber matrix during reacting with ZnO to form zinc stearate.

The mechanism of controlling the mesh size in series 2 is also explained by the generation of zinc stearate, which may further form active complexes with sulfur and CBS.[1−5,50] The increase of ZnO is thought to increase the generation of zinc stearate in the rubbery matrix when an enough amount of stearic acid is mixed. The increment would promote the sulfur cross-linking reaction, followed by the increase of the cross-linking in the matrix to result in the decrease of mesh size. However, an excess of ZnO against stearic acid did not give a variation of the mesh size, which may be ascribable to almost the same concentration of zinc stearate in the both rubber matrixes of the samples mixed with ZnO of 2.0 phr and 4.0 phr. ZnO of 2.0 phr would be enough to react with stearic acid of 2.0 phr to generate zinc stearate in our recipe shown in Table 1.

On the other hand, the mechanism of formation of network domain in series 2 is explained as follows: Sulfur and CBS are adsorbed on ZnO as mentioned in the previous section. Thus, the increase of ZnO under the definite amounts of stearic acid, sulfur, and CBS seems to decrease the adsorbed amounts of these cross-linking reagents per ZnO cluster. The decrease of the absorbed amounts would result in the smaller Ξ value due to the lower degree of vulcanization reactions around each ZnO cluster.

Then, why did a large amount of ZnO give no change in the size of network domain as shown in the case of 4.0 phr of ZnO? Possibly, a byproduct or the final product of vulcanization reactions, ZnS, may have brought about similar results in IR-2-Z2-St2 and in IR-2-Z4-St2. Taking into account the difference of scattering length densities of constituents with that of *d*-toluene,[55] the observed inhomogeneous domains detected by SANS are considered to contain the dispersed area of ZnS particles where sulfur−sulfur bonds were possibly formed as shown in a schematic picture in Figure 2b.

The similar Ξ values between IR-2-Z2-St2 and IR-2-Z4-St2 suggest a similar degree of the sulfur cross-linking reactions, resulting in a similar dispersion area of ZnS after the vulcanization. Thus, the size of ZnO clusters should be smaller than that of dispersion area of ZnS, because the amount of ZnO of IR-2-Z4-St2 was double against that of IR-2-Z2-St2. Unreacted sulfur and CBS may remain around ZnO and ZnS clusters. The total area of network domains shown in Figure 2b leads to the upturn scatterings at low q region in this study. The similar Ξ values also suggest that stearic acid gave a dispersion effect to ZnO, and consequently the ZnO clusters in the rubbery matrix are similar between the samples mixed with ZnO of 2.0 phr and 4.0 phr (IR-2-Z2-St2 and IR-2-Z4-St2).

Up to now, ZnO particles have been believed to work also as reinforcing filler,[56] even if the effect is less than that of carbon black. However, the morphological structure of ZnO particles has not been clarified at all. Our SANS results may provide an answer: The structure shown in Figure 2b is an origin of its reinforcement effect, where the polyisoprene network covers ZnO clusters and many ZnS particles dispersed in the network domains. This specific feature of the network domain may give a different and/or weaker reinforcement effect than carbon black that has a bound rubber layer (due to chemisorption) on its surface.[49,57−59] Certainly, it should be kept in mind that a dried state of vulcanizates is more shrunken than the swollen state shown in Figure 2.

Effect of Network Inhomogeneity on SIC. Fundamentally, rubber is practically utilized under the dynamic conditions, where rubber is stretched and retracted repeatedly. Then, what is the effect of the inhomogeneity of network structure on the mechanical properties of the cross-linked IR? There are no quantitative reports on the relationship between the inhomogeneity of network structure and properties of cross-linked rubbers. In order to reveal the effects of inhomogeneity of network on the properties, a specific feature of strain-induced crystallization (SIC) behaviors of cross-linked IR is considered in this study. It is notable that the SIC is reversible, i.e., melting of the crystallites are observed on retraction,[21,32,33] though the results on contraction are not presented here.

Figure 4 shows tensile stress−strain curves up to the mechanical rupture points of all samples, where the plotted points show the event of X-ray irradiation for WAXD measurements. For all series, the larger is the network-chain density, the higher is the stress at any stretching ratio, and an upturn of tensile stress is observed at the intermediate strain region. The slope after the upturn tended to become larger with the increase of the network-chain density in all series except IR-2-Z4-St2. From the viewpoint of the inhomogeneity of networks, on the other hands, it is revealed in this study that the stress increased with an increase of size of the network domains in series 1 even though the mesh sizes of the samples were similar. For series 2, the stress was found to increase with the decrease of size of the network domains when the mesh size decreased accordingly. Probably, the number of the network domains affects the tensile properties. A similar inhomogeneity in the networks brought

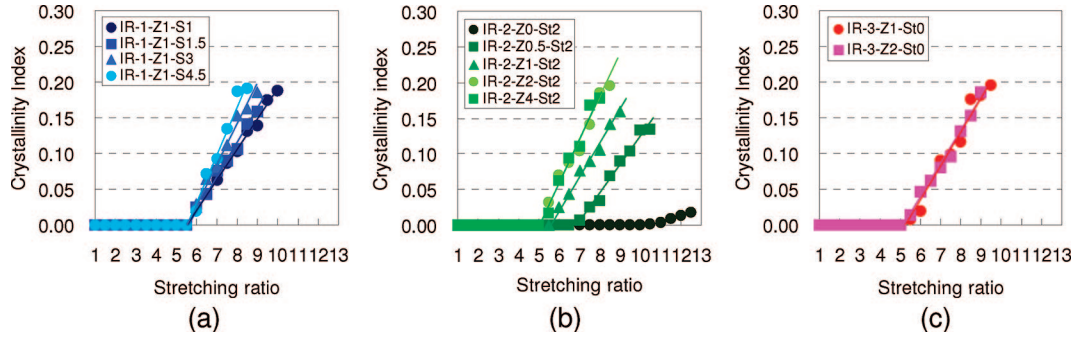

Figure 5. Relationship between crystallinity index and stretching ratio of IR vulcanizates: (a) series 1, (b) series 2, and (c) series 3 samples.

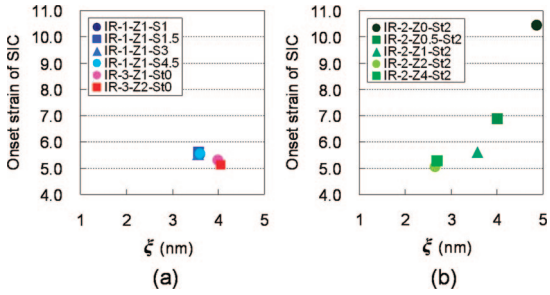

Figure 6. Relationship between onset strain of SIC and ξ: (a) series 1 and series 3, and (b) series 2 samples. Colors of the data points show the samples corresponding to those in Figures 4 and 5.

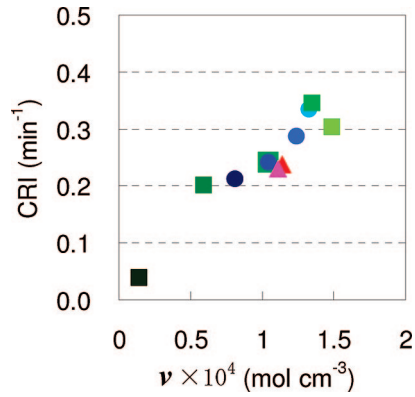

Figure 7. Relationship between CRI and ν. Colors of the data points show the samples corresponding to those in Figures 4 and 5.

to similar tensile characteristics as shown in series 3.

Figure 5a shows the crystallinity index of series 1 plotted against stretching ratio. Note that the onset of the strains of SIC of series 1 samples were almost equal regardless of their network-chain densities, while the rate of crystal growth by SIC increased by increasing the network-chain density. These facts have already been reported in several papers,[22−24,32] but it has been a question what governs the onset strain. The present results of SANS give an answer: Almost the same mesh size in the rubbery matrix has resulted in similar onset strains for the cross-linked IR of series 1. The crystallization occurred mainly in the rubbery matrix, but not much inside the network domain phase. Consequently, crystallizable segments upon stretching are identified to be network chains in the rubbery matrix, i.e., the A phase of the inhomogeneous two-phase model (see Figure 2a). These conjectures are supported by the results of SIC of series 2 and 3. The onset strains of series 2 decreased with the increase of ZnO, *i.e.*, the decrease of mesh size up to 2.0 phr of ZnO, whereas those of IR-2-Z2-St2 and IR-2-Z4-St2 were almost the same as shown in Figure 5b. Also, the onset strains of series 3 except IR-3-Z4-St0[60] were almost equal to each other as shown in Figure 5c in accord with the similar mesh size in the networks. The correlation between the mesh size ξ and the onset strain of SIC is plotted in Figure 6, parts a (series 1 and 3) and b (series 2).

When the relative crystallization rate index (CRI) is compared among the samples of series 1, the increase of Ξ was found to result in the increase of CRI. Rigid network domains promoted SIC of isoprene segments in the rubbery matrix. In series 2, however, CRI increased in spite of the decrease of Ξ. For the CRI of series 2, the decrease of mesh size and the increase of number of network domains seem to affect CRI more effectively. It is worth noting, here, that CRI is found to be correlated with the "overall" network-chain density, and the increase results in an increase of CRI in all samples as shown in Figure 7, where the network-chain density (ν) evaluated by tensile experiments are plotted. In a long history of rubber elasticity, though many physical properties have been discussed from the overall network-chain density of the materials, the inhomogeneity of the networks has not been taken into account. This might have been one of the reasons why the physics and properties of vulcanized rubbers have not been fully elucidated yet. In other words, not only the morphology of inhomogeneous structure but also the network chain density in each phase must be considered, together with the overall network-chain density for the further development of rubber science. More detail discussions on the relationship between the inhomogeneous network structures and SIC behaviors of the samples will be reported in a forthcoming paper.

Conclusion

Network inhomogeneity of the swollen IR vulcanizates was characterized by SANS measurements. The inhomogeneity control of domains with high network-chain densities are embedded in rubbery network matrix. Polyisoprene networks surround ZnO clusters and many ZnS particles disperse in the network domains. Unreacted sulfur and accelerator may exist near ZnO particles or its clusters depending on the curing conditions. We also found a new aspect of the vulcanization to determine mesh size (ξ) and size of network domain (Ξ) in the cross-linked rubber. The following mechanism is proposed for the inhomogeneity control of network structures in vulcanization in the presence of stearic acid of 2.0 phr, which is schematically illustrated in Figure 8. Here, the cartoons were drawn in order to emphasize only the difference of essential roles of vulcanizing reagents for controlling the mesh size and network domains. In reality, however, ξ and Ξ should be referred to the measured mesh size and size of network domains shown in Table 1.

Upon heat-pressing rubber compounds, stearic acid is reacted with ZnO to form solubilized zinc stearate in the rubbery matrix. Generated zinc stearate is reacted with sulfur and accelerator in the rubbery matrix to form sulfur cross-links. Thus, the concentration of zinc stearate is one of the factors to control

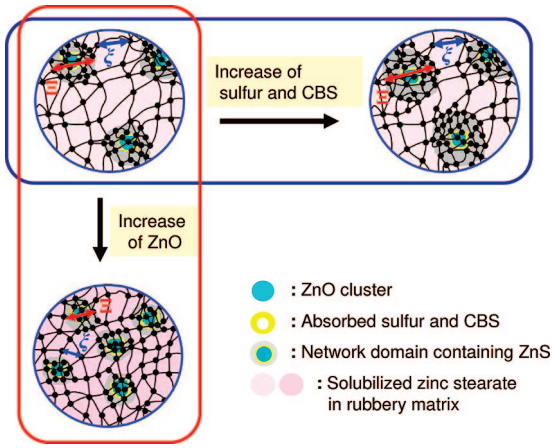

Figure 8. Schematic presentation of the formation of two-phase inhomogeneity in rubber vulcanizates on the basis of the amounts of sulfur, CBS (accelerator) and ZnO in the presence of stearic acid of 2 phr.

the mesh size in the matrix. On the other hand, sulfur and accelerator are adsorbed on the remaining ZnO clusters, which are dispersed in the rubbery matrix, followed by sulfur cross-linking on the surface area of ZnO clusters. Thus, the amounts of sulfur and accelerator relative to that of ZnO become important in the presence of stearic acid of 2.0 phr in controlling the size of network domains. In this connection, it should be kept in mind that the variation of sulfur cross-linking reagents in the vulcanization can be quite various, and the results described in this paper are characteristics of one of the representative vulcanization systems. The observed network inhomogeneity, however, well explains the characteristic feature of strain-induced crystallization of vulcanizates. The crystallization is found to occur mainly in the rubbery matrix, but not much inside the network domain phase.

The present observations and their analytical results will open a new window for further developing of vulcanization process. For example, the results on ZnO are useful for considering its substitute: Zinc released from tires by wear is a problematic environmental pollutant.[61]

Acknowledgment. This work was supported by the Ogasawara Foundation for the Promotion of Science & Engineering and by KIT to Y.I. and by the Ministry of Education, Science, Sports and Culture, Japan (Grant-in-Aid 18205025) to M.S. The SANS experiment was performed with the approval of Institute for Solid State Physics, The University of Tokyo (Proposal No. 7623), at Japan Atomic Energy Research Institute Agency, Tokai, Japan. The synchrotron radiation experiment on WAXD was performed at the BL-40XU in the SPring-8 with the approval of the Japan Synchrotron Radiation Research Institute (JASRI) (Proposal No. 2007A1933). The authors thank to Messrs H. Komori, K. Utani, Y. Kasahara, and Y. Yasuda and Dr. Y. Yuguchi for their active assistance in conducting experiments.

References and Notes

(1) Coran, A. Y. In *Science and Technology of Rubber*, 2nd ed.; Mark, J. E., Erman, B., Eirich, F. R., Eds., Academic Press, San Diego, 1994; Chapter 7, pp339−385.
(2) Bateman, L.; Moore, C. G.; Porter, M.; Saville, B. In *The Chemistry and Physics of Rubber-like Substances*; Bateman, L., Ed., MacLaren & Sons: London, 1963, Chapter 15, pp449−561.
(3) Chapman, A. V.; Porter, M. In *Natural Rubber Science and Technology*; Roberts, A. D., Ed., Oxford University Press: Oxford, U.K., 1988, Chapter 12, pp 511−620.
(4) Coran, A. Y. *Rubber Chem. Technol.* **1965**, *38*, 1–14.
(5) Coran, A. Y. *J. Appl. Polym. Sci.* **2003**, *87*, 24–30.
(6) Stein, R. S. *J. Polym. Sci., Polym. Lett. Ed.* **1969**, *7*, 657–660.
(7) Shibayama, M. *Macromol. Chem. Phys.* **1998**, *199*, 1–30.
(8) Bastide, J.; Duplessix, R.; Picot, C.; Candau, S. *Macromolecules* **1984**, *17*, 83–93.
(9) Higgins, J. S.; Benoit, H. C. *Polymers and Neutron Scattering*; Clarendon Press: Oxford, U.K., 1994.
(10) Archer, B. L.; Barnard, D.; Cockbain, E. G.; Dickenson, P. B.; McMullen, A. I. In *The Chemistry and Physics of Rubber-like Substances*; Bateman, L., Ed.; MacLaren & Sons: London, 1963; Chapter 3, pp 41−72.
(11) Wititsuwannakul, D.; Wititsuwannakul, R. In *Biopolymers*, Steinbuchel, A. Ed.; Wiley-VCH: Weinheim, Germany, 2001; Vol. 2, Chapter 6, pp 151−202.
(12) Karino, T.; Ikeda, Y.; Yasuda, Y.; Kohjiya, S.; Shibayama, M. *Biomacromolecules* **2007**, *8*, 693–699.
(13) Candau, S.; Bastide, J.; Delsanti, M. *Adv. Polym. Sci.* **1982**, *44*, 27–71.
(14) Dusek, K.; Prins, W. *Adv. Polym. Sci.* **1969**, *6*, 1–102.
(15) Shibayama, M. *Bull. Chem. Soc.* **2006**, *79*, 1799–1819.
(16) Shibayama, M.; Tanaka, T.; Han, C. C. *J. Chem. Phys.* **1992**, *97*, 6829–6841.
(17) Horkay, F.; McKenna, G. B.; Deschamps, P.; Geissler, E. *Macromolecules* **2000**, *33*, 5215–5220.
(18) Karino, T.; Okumura, Y.; Zhao, C.; Kataoka, T.; Ito, K.; Shibayama, M. *Macromolecules* **2005**, *38*, 6161–6167.
(19) Matsunaga, T.; Sasaki, T.; Akagi, Y.; Chung, U.; Shibayama, M. *Macromolecules* **2009**, *42*, 1344–1351.
(20) http://www.spring8.or.jp/j/.
(21) Murakami, S.; Senoo, K.; Toki, S.; Kohjiya, S. *Polymer* **2002**, *43*, 2117–2120.
(22) Ikeda, Y.; Yasuda, Y.; Makino, S.; Yamamoto, S.; Tosaka, M.; Senoo, K.; Kohjiya, S. *Polymer* **2007**, *48*, 1171–1175.
(23) Tosaka, M.; Senoo, K.; Kohjiya, S.; Ikeda, Y. *J. Appl. Phys.* **2007**, *101*, 084909/1−084909/8.
(24) Ikeda, Y.; Yasuda, Y.; Hijikata, K.; Tosaka, M.; Kohjiya, S. *Macromolecules* **2008**, *41*, 5876–5884.
(25) http://www.sakai-chem.co.jp/product/muki_aen.html.
(26) Kohjiya, S.; Tosaka, M.; Furutani, M.; Ikeda, Y.; Toki, S.; Hsiao, B. S. *Polymer* **2007**, *48*, 3801–3808.
(27) Okabe, S.; Nagao, M.; Karino, T.; Watanabe, S.; Adachi, T.; Shimizu, H.; Shibayama, M. *J. Appl. Crysallogr.* **2005**, *38*, 1035–1037.
(28) Okabe, S.; Karino, T.; Nagao, M.; Watanabe, S.; Shibayama, M. *Nucl. Instrum. Methods Polym. Res., A* **2007**, *572*, 853–858.
(29) Shibayama, M.; Nagao, M.; Okabe, S.; Karino, T. *J. Phys. Soc. Jpn.* **2005**, *74*, 2728–2736.
(30) Hahn, T. *Int. Tables Crystallogr.* **1983**, 157.
(31) Toki, S.; Sics, I.; Ran, S.; Liu, L.; Hsiao, B. S.; Murakami, S.; Senoo, K.; Kohjiya, S. *Macromolecules* **2002**, *35*, 6578–6584.
(32) Tosaka, M.; Murakami, S.; Poompradub, S.; Kohjiya, S.; Ikeda, Y.; Toki, S.; Sics, I; Hsiao, B. S. *Macromolecules* **2004**, *37*, 3299–3309.
(33) Tosaka, M.; Kohjiya, S.; Murakami, S.; Poompradub, S.; Ikeda, Y.; Toki, S.; Sics, I.; Hsiao, B. S. *Rubber Chem. Technol.* **2004**, *77*, 711–723.
(34) Flory, P. J. *J. Chem. Phys.* **1950**, *18*, 108–111.
(35) Barton, A. F. M. In *Handbook of Polymer-Liquid Interaction Parameters and Solubility Parameters*; CRC Press: Boca Raton, FL, 1990; Part II, p 248.
(36) χ of 0.39 was used for the calculation, which was an average χ for polyisoprenes/toluene pair at temperature below 50°C. In rubber technology, χ of 0.393 for the natural rubber/toluene pair at 25 °C. (Brisrow, G. M.; Watson, W. F. *Trans. Faraday Soc.* **1958**, *54*, 1567–1573. Wagner, H. L.; Flory, P. J. *J. Am. Chem. Soc.* **1952**, *74*, 195–200) has been often utilized for the evaluation of ν of IR vulcanizates. Since swelling experiments was reported to only yield a qualitative approximation to the real network-chain density of the natural rubber vulcanizates (Valentín, J. L.; Carretero-González, J.; Mora-Barrantes, I.; Chassé, W.; Saalwächter, K. *Macromolecules* **2008**, *41*, 4714–4729.) the determination of network-chain density was also conducted on the basis of the classical theory of rubber elasticity[37] in this study. A specific inhomogeneity of rubber vulcanizates shown later may be ascribable to the uncertainties in the determination of network-chain density by equilibrium swelling experiments.
(37) Treloar, L. R. G. *The Physics of Rubber Elasticity*; Clarendon Press: Oxford, U.K., 1975.
(38) de Gennes, P. G. *Scaling Concepts in Polymer Physics*; Cornell Univ.: Ithaca, NY, 1979.
(39) Mallam, S.; Hecht, A.-M.; Geissler, E.; Pruvost, P. *J. Chem. Phys.* **1989**, *91*, 6447–6454.
(40) Mallam, S.; Horkay, F.; Hecht, A.-M.; Rennie, A. R.; Geissler, E. *Macromolecules* **1991**, *24*, 543–548.
(41) Horkay, F.; Hecht, A.-M.; Mallam, S.; Geissler, E. *Macromolecules* **1991**, *24*, 2896–2902.
(42) Onuki, A. *J. Phys. II Fr.* **1992**, *2*, 45–61.

(43) Shibayama, M.; Takahashi, H.; Nomura, S. *Macromolecules* **1995**, *28*, 6860–6864.
(44) Shibayama, M.; Isono, K.; Okabe, S.; Karino, T.; Nagao, M. *Macromolecules* **2004**, *37*, 2909–2918.
(45) Wu, W.; Shibayama, M.; Roy, S.; Kurokawa, H. Z.; Coyen, L. D.; Nomura, S.; Stein, R. S. *Macromolecules* **1990**, *23*, 2245–2251.
(46) Soni, V. K.; Stein, R. S. *Macromolecules* **1990**, *23*, 5257–5265.
(47) Debye, P.; Bueche, A. M. *J. Appl. Phys.* **1949**, *20*, 518–525.
(48) Fujimoto, K. *Nippon Gomu Kyokaish* **1964**, *37*, 602–619.
(49) Kato, A.; Kohjiya, S.; Ikeda, Y. *Rubber Chem. Technol.* **2007**, *80*, 690–700.
(50) Manik, S. P.; Banerjee, S. *Rubber Chem. Technol.* **1969**, *42*, 744–758.
(51) Heideman, G.; Datta, R. N.; Noordermeer, J. W. M.; Van Baarle, B. *J. Appl. Polym. Sci.* **2005**, *95*, 1388–1404.
(52) Steudel, R.; Steudel, Y. *Chem. Eur. J.* **2006**, *12*, 8589–8602.
(53) Dohi, H.; Horiuchi, S. *Polymer* **2007**, *48*, 2526–2530.
(54) Horiuchi, S.; Dohi, H. *Langmuir* **2006**, *22*, 4607–4613.
(55) (a) Bacon, G. E. *Neutron Diffraction*, 3rd ed.; Clarendon Press, Oxford, U.K., 1975. Calculated scattering length densities: ZnO, 4.8×10^{10} cm^{-2}; ZnS, 2.1×10^{10} cm^{-2}; *N*-cyclohexyl-2-benzothiazole sulfenamide (CBS), 1.5×10^{10} cm^{-2}; S_8, 1.1×10^{10} cm^{-2}; isoprene rubber, 2.7×10^{9} cm^{-2}; stearic acid, -6.6×10^{8} cm^{-2}; zinc stearate, -9.2×10^{7} cm^{-2}; *d*-toluene, 5.7×10^{10} cm^{-2}.
(56) Park, C. R. *Ind. Eng. Chem.* **1939**, *31*, 1402–1406.
(57) Donnet, J.-B.; Bansal, R. C., Wang, M.-J.; *Carbon Black*, Marcel Dekker; New York, 1993.
(58) Kohjiya, S.; Katoh, S.; Shimanuki, J.; Hasegawa, T.; Ikeda, Y. *J. Mater. Sci.* **2005**, *40*, 2553–2555.
(59) Kohjiya, S.; Katoh, A.; Suda, T.; Shimanuki, J.; Ikeda, Y. *Polymer* **2006**, *47*, 3298–3301.
(60) Determination of crystallinity index of IR-3-Z4-St0 was not done, because the significant WAXD patterns of ZnO were recognized due to the large amount and the absence of stearic acid.
(61) Chapman, A.; Johnson, T. *Kautsch. Gummi Kunstst.* **2005**, *58*, 358–361.

MA802730Z